Chinese Journal of Electronics
vol. 33, no. 5, pp. 1188–1195, September 2024
https://doi.org/10.23919/cje.2023.00.087

CJE

RESEARCH ARTICLE

Study on Static Deflection Model of MEMS Capacitive Microwave Power Sensors

Ye JIN[1] and Debo WANG[2]

1. *College of Electronic and Optical Engineering* & *College of Flexible Electronics* (*Future Technology*), *Nanjing University of Posts and Telecommunications*, *Nanjing 210023*, *China*
2. *College of Integrated Circuit Science and Engineering*, *Nanjing University of Posts and Telecommunications*, *Nanjing 210023*, *China*

Corresponding author: Debo WANG, Email: wdb@njupt.edu.cn
Manuscript Received April 2, 2023; Accepted October 27, 2023
Copyright © 2024 Chinese Institute of Electronics

Abstract — In this paper, a static deflection model of MEMS cantilever beam is proposed, which can better study the force deformation of micro-electro-mechanical system (MEMS) cantilever beam and the output characteristics of capacitive microwave power sensor. The deflection curve is used to describe the deformation of the cantilever beam and then the overload power and sensitivity of this power sensor are derived. It is found that the overload power decreases with the beam length, and increases with the initial height of beam. The sensitivity increases with the beam length, and has a linear growth relationship with the measuring electrode width. A MEMS dual-channel microwave power sensor is designed, fabricated and measured. At a microwave signal frequency of 10 GHz, the sensitivity of the sensor is measured to be 0.11 V/W for the thermoelectric detection channel and 65.17 fF/W for the capacitive detection channel. The sensitivity calculated by the lumped model is 92.93 fF/W, that by the pivot model is 50.88 fF/W, and that by the deflection model proposed in this work is 75.21 fF/W. Therefore, the theoretical result of the static deflection model is more consistent with the measured result and has better accuracy than the traditional lumped model and pivot model.
Keywords — Micro-electro-mechanical system (MEMS) cantilever beam, Static deflection model, Power sensor, Overload power, Sensitivity.
Citation — Ye JIN and Debo WANG, “Study on Static Deflection Model of MEMS Capacitive Microwave Power Sensors,” *Chinese Journal of Electronics*, vol. 33, no. 5, pp. 1188–1195, 2024. doi: 10.23919/cje.2023.00.087.

I. Introduction

In recent years, micro-electro-mechanical system (MEMS) technology has developed rapidly, and MEMS microwave power sensors have also played an increasingly important role in power detection [1], [2]. The widely used microwave power sensors are mainly divided into thermoelectric type and capacitive type. Thermoelectric microwave power sensors were proposed by Dehé *et al.* [3] in 1995. The sensor was fabricated using GaAs/AlGaAs technology, which can achieve a sensitivity of 1.1 V/W. In 2010, Wang *et al.* [4] designed an amplification system for the thermoelectric microwave power sensor, which can well amplify the output of the weak signal of the power sensor, and the sensitivity is 0.24 mV/mW at 10 GHz. In 2015, Zhang *et al.* [5] studied the temperature distribution of indirectly heated thermoelectric microwave power sensors to achieve good signal-to-noise ratio (SNR). In 2019, Chu *et al.* [6] designed an X-band MEMS thermoelectric power sensor with a sensitivity of 82.5 mV/W, which integrated a power divider into the chip to achieve integrated detection of power, frequency, and phase. In 2021, Li *et al.* [7] designed a new MEMS power sensor based on a double-layer thermocouple with high sensitivity and large dynamic range. He introduced a root mean square (RMS) microwave thermoelectric power detector with a sensitivity of 3.27 μV/mW at 10 GHz in 2022 [8]. Generally, the thermoelectric microwave power sensor has good linearity, and does not need additional direct current (DC) bias. However, its disadvantage is that the thermopile is easy to overheat and burn when detecting high power, which is only applicable to low power detection.

In order to achieve online detection and improve the

Associate Editor: Prof. Jinjun FENG, Beijing Vacuum Electronics Research Institute, China Electronics Technology Group Corporation.

overload power, the capacitive microwave power sensor has become a research hotspot. In 2006, Fernández *et al.* [9] designed a capacitive microwave power sensor with a MEMS beam, whose sensitivity was 90 aF/mW, realizing the online detection of microwave power. In 2011, Cui *et al.* [10] proposed a new MEMS microwave power sensor, which consisted of a linear gradient signal line and ground to avoid step discontinuity. At the same year, Yi *et al.* [11] designed a capacitive microwave power detection system by using a MEMS cantilever structure, whose sensitivity was 6 aF/mW, and a static lumped model of the cantilever beam was proposed, but the parameters of the cantilever beam were not optimized, and there was a large error between the theoretical value and the measured value. In 2015, Yan *et al.* [12] studied the high overload power characteristics of a capacitive microwave power sensor with a grounded MEMS beam. They divided the measurements into three regions: linear, transition, and saturation. In 2020, Zuo *et al.* [13] established a static pivot model of capacitive MEMS microwave power sensor to optimize the relative position of the measuring electrode, but the pivot model was still not accurate enough. In 2022, in order to improve the sensitivity characteristics and reliability, Li *et al.* [14] proposed a new capacitive power sensor based on dual MEMS cantilever, which used the lumped model to study the capacitive power sensor.

In recent years, a dual-channel microwave power sensor and its model were studied [15]–[17], which had the advantages of both good linearity of thermoelectric sensors and high overload power of capacitive sensors. In 2012, Wang *et al.* [16] proposed a novel MEMS dual-channel microwave power sensor based on GaAs MMIC (monolithic microwave integrated circuit) technology. Thermoelectric and capacitive microwave power sensors were integrated in that work. The static lumped model is established to study its sensitivity, but the lumped model is inaccurate. In 2015, Kosobutskyy *et al.* [17] equated the cantilever beam as an oscillation system with concentrated elastic and inertial parameters, and optimized the geometric dimensions of the cantilever beam. In 2016, Yi *et al.* [18] proposed a novel cascaded terminal-type and capacitive power sensor, with a terminal-type thermoelectric power sensor designed for low-power detection and a capacitive power sensor designed for high-power detection. In 2019, Kasambe *et al.* [19] proposed a stepped cantilever beam based on variable width to reduce the pull-in potential, and mathematically modeled this unconventional cantilever using the conjugate beam method. In the same year, Singh *et al.* [20] proposed an electromechanically coupled macroscopic model of MEMS cantilever beams for electrostatic actuation.

In summary, the previous studies on the mechanical characteristics of MEMS beams in capacitive microwave power sensors or capacitive channels of dual-channel microwave power sensors are mostly used with lumped models or pivot models, but the morphology description of cantilever beam during operation by these two models is inaccurate. The lumped model assumes that the pull-down displacements of the cantilever beam are equal everywhere, but in fact, when the beam is subjected to the electrostatic attraction of the signal line, the degree of deformation is different everywhere, that is, the pull-down displacement is not equal. This will lead that the theoretical results of overload power and sensitivity is not accurate. The pivot model assumes that the cantilever beam is a rigid plate rotating around the fixed end, and that the pull-down displacement at each point of the beam is linearly related to the horizontal distance from the fixed end to each point. However, the two are nonlinear. If they are considered to be linear, the theoretical capacitance values will be inaccuracy. Therefore, a MEMS cantilever beam static deflection model based on the bending curve equation is proposed in this work, by which the deformation of the cantilever beam can be described more accurately. The free end of the cantilever beam is electrostatically attracted by the signal line, due to the self-elasticity of the beam, the pull-down displacement at each point has a nonlinear relationship with the horizontal distance from the fixed end. Based on this static deflection model, the theoretical results of capacitance, overload power and sensitivity are more accurate.

II. Principle and Model

Taking into account the advantages of good linearity of thermoelectric microwave power sensor and high overload power of capacitive microwave power sensor, a MEMS dual-channel microwave power sensor is designed as shown in Figure 1. It is composed of coplanar waveguide (CPW), MEMS cantilever beam, measuring electrode, thermopile, load resistor, output pad, and GaAs substrate. The MEMS cantilever beam is located directly above CPW and the measuring electrode. The load resistor is located at the termination of CPW, and adjacent to the thermopile.

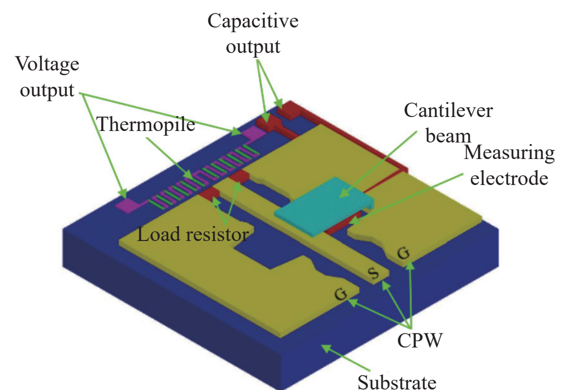

Figure 1 Structure of MEMS dual-channel microwave power sensor.

The thermoelectric power sensor consists of thermopiles, two load resistors and CPW. When the input microwave power is low, the load resistor will convert almost all of the microwave power into heat, causing the

temperature of thermopile around the load resistor to rise at one end and producing a temperature difference with the other end. According to the Seebeck effect, the input signal power can be measured by measuring output DC electric potential.

The capacitive power sensor is composed of a CPW, a MEMS cantilever beam and a measuring electrode. When the input microwave power is high, the MEMS cantilever beam is deformed by the electrostatic attraction, and the capacitance between the test electrode and the cantilever changes. Therefore, the sensor will output capacitance change which is proportional to input signal power.

1. Overload power analysis

When the input power is high, the capacitive type couples most of the power, and only a small part of the power is transmitted to the thermoelectric type. Therefore, the overload power of the dual-channel sensor is mainly decided by that of the capacitive sensor. The structural parameters of capacitive detection channel are shown in Table 1. The static deflection model of the MEMS cantilever beam is studied as shown in Figure 2. F_e is the attraction of signal line to the beam, L is the length of beam, t is the thickness of beam, g_0 is the initial spacing of beam, δ is the spacing between CPW and the free end of the beam, and $\omega(x)$ is the spacing (deflection) between the beam and CPW or test electrode at x. To make the derivation process simpler, let $x_i = c_i \times L$.

Table 1 Structural parameters of capacitive detection channel

Symbol	Description	Value
E	Young's modulus of cantilever beam (Au)	79.42 GPa
ε_0	Permittivity of air	8.85×10^{-12} F/m
Z_0	Impedance of matched load	50 Ω
L	Length of cantilever beam	308 μm
g_0	Initial height of cantilever beam	1.6 μm
t	Thickness of cantilever beam	2 μm
b_1	Width of cantilever beam	240 μm
b_2	Width of test electrode	200 μm
x_1	Horizontal distance between the left end of test electrode and the fixed end of cantilever beam	8 μm
x_2	Horizontal distance between the right end of test electrode and the fixed end of cantilever beam	208 μm
x_3	Horizontal distance between the left end of signal line and the fixed end of cantilever beam	218 μm

Because the signal line has the electrostatic attraction to the cantilever beam, F_e acts on $[x_3, L]$. Assuming the unit load of this force is q, and the electrostatic attraction can be expressed as

$$F_e = q\cdot(L-x_3) = q(1-c_3)L \tag{1}$$

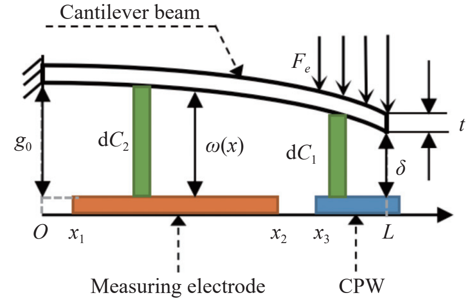

Figure 2 Static deflection model of MEMS cantilever.

In order to obtain the deflection of the beam, firstly, according to the force of the beam, the bending moment is expressed as shown in (2). Secondly, the bending moment expression is substituted and integrated into the small deflection differential equation as shown in (3). Thirdly, the constraint and continuity conditions as shown in (4) are used to determine the integration constants. Finally, the deflection equation of the beam is got as shown in (5).

$$M(x) = \begin{cases} q(L-x_3)\left(x-\dfrac{x_3+L}{2}\right), & 0\le x\le x_3 \\ \dfrac{q}{2}(L-x)^2, & x_3\le x\le L \end{cases} \tag{2}$$

$$EI\frac{\mathrm{d}^2\omega(x)}{\mathrm{d}x^2} = M(x) \tag{3}$$

$$\begin{cases} \omega(0)=0 \\ \omega'(0)=0 \\ \omega(x_3^-)=\omega(x_3^+) \\ \omega'(x_3^-)=\omega'(x_3^+) \end{cases} \tag{4}$$

where $M(x)$ is the bending moment of the cantilever beam, $I=b_1\times t^3/12$ is the rotational inertia of the cantilever beam, $\omega(x)$ is the deflection of the beam at x, and $\omega'(x)$ is the rotation angle of the beam at x.

Since the deflection equation is a 4th order equation, the solution process is tedious. To facilitate the calculation, $x_3 = (218/308)\times L = 0.7078\times L$ is substituted to obtain the deflection equation of the beam in (5).

$$\omega(x) = \frac{q}{EI}\cdot\begin{cases} -0.0487L\cdot(x-0.854)^3+0.107L^3x \\ \quad -0.0303L^4, \qquad 0\le x\le x_3 \\ \dfrac{1}{24}(L-x)^4+0.108L^3x-0.0312L^4, \\ \qquad x_3\le x\le L \end{cases} \tag{5}$$

δ is the distance between the free end of cantilever beam and CPW, which can be expressed by the deflection equation as the deflection $\omega(L)$, as shown in (6). Let $x = a\times L$, associative (6), the deflection equation can be expressed as a function of δ and a as shown in (7). In this work, the relative value of the signal line position compared with the beam length is used instead of representing the absolute value of the signal line position,

which can be easily calculated without affecting the universality of the model.

$$\delta = \omega(L) = \frac{q}{EI} \cdot 0.0764L^4 \quad (6)$$

$$\omega(a) = \delta \cdot \begin{cases} f_1(a), & 0 \le a \le c_3 \\ f_2(a), & c_3 \le a \le 1 \end{cases} = \frac{\delta}{0.0764} \cdot \begin{cases} -0.0487(a-0.854)^3 + 0.107a \\ \quad -0.0303, & 0 \le a \le c_3 \\ \frac{1}{24}(1-a)^4 + 0.108a - 0.0312, \\ & c_3 \le a \le 1 \end{cases} \quad (7)$$

In the horizontal direction, take the length microelement $\mathrm{d}x$, in which case the capacitance between the signal line and the cantilever beam can be regarded as the capacitance of plate capacitor, as shown in (8).

$$\mathrm{d}C_1 = \frac{\varepsilon_0 b_1 \mathrm{d}x}{g_0 + \frac{g_1}{\varepsilon_r} - \omega(x)} \quad (8)$$

where b_1 is the width of the cantilever beam, ε_0 and ε_r are the relative permittivity of air and the oxide dielectric layer, and g_1 is the thickness of the oxide dielectric layer above the electrode.

Due to $g_1 \ll g_0$, $\varepsilon_r \gg 1$, equation (8) can be rewritten as (9). According to electrical theory, the relationship of electrostatic force with capacitance can be expressed as (10).

$$\mathrm{d}C_1 = \frac{\varepsilon_0 b_1 L \mathrm{d}a}{g_0 - \omega(a)} \quad (9)$$

$$\mathrm{d}F_e = \frac{1}{2}\left|\frac{\partial(\mathrm{d}C_1)}{\partial\delta}\right| V^2 = \frac{\varepsilon_0 b_1 L V^2}{2} \cdot \frac{f_2(a)\mathrm{d}a}{(g_0 - \delta\cdot f_2(a))^2} \quad (10)$$

where V is the input voltage of the microwave signal.

The electrostatic attraction acts on $[x_3, L]$, and the integral of (10) gives an expression of F_e as shown in (11). According to (1) and (6), equation (12) is obtained. According to (11) and (12), equation (13) is obtained. According to electrical theory, the input power of the sensor is related to the drive voltage and the matched impedance Z_0, expressed as (14).

$$F_e = \int_{c_3}^{1} \frac{\varepsilon_0 b_1 L V^2}{2} \cdot \frac{f_2(a)}{(g_0 - \delta\cdot f_2(a))^2}\mathrm{d}a \quad (11)$$

$$F_e = \frac{EI}{0.07636L^4} \cdot \delta \cdot (1-c_3)L \quad (12)$$

$$V^2 = \frac{2EI(1-c_3)}{0.0764\varepsilon_0 L^4 b_1} \cdot \frac{\delta}{\int_{c_3}^{1} \frac{f_2(a)}{(g_0 - \delta\cdot f_2(a))^2}\mathrm{d}a} \quad (13)$$

$$P_{\mathrm{in}} = \frac{V^2}{Z_0} = \frac{2EI(1-c_3)}{0.0764Z_0\varepsilon_0 L^4 b_1} \cdot \frac{\delta}{\int_{c_3}^{1} \frac{f_2(a)}{(g_0 - \delta\cdot f_2(a))^2}\mathrm{d}a} \quad (14)$$

As the microwave power of the input signal increases, the MEMS beam will gradually approach the CPW, and when the input microwave power reaches a certain value, the system composed of beam and CPW enters a critical equilibrium state. In this state, if the microwave power continues to increase, the beam and the CPW transmission line will suddenly absorb together due to the nonlinear behavior of the MEMS beam. The phenomenon is the pull-in phenomenon, the equilibrium position point is called pull-in point and the corresponding displacement is called pull-in displacement. The input power at the pull-in point reaches the maximum, which is called the overload power. According to (14) and (15), equation (16) is obtained. Substituting (16) into (14), equation (17) is obtained.

$$\frac{\partial P_{\mathrm{in}}}{\partial \delta} = 0 \quad (15)$$

$$\delta_{\text{pull-in}} = 0.398g_0 \quad (16)$$

$$P_{\mathrm{overload}} = \frac{0.493Et^3 g_0^3}{\varepsilon_0 Z_0 L^4} \quad (17)$$

The results show that the overload power of the capacitive channel is closely related to the length, thickness and initial height of the beam. The relationship between the overload power and the initial height and length of the beam is shown in Figure 3 as the thickness of the beam is 2 μm. The overload power is negatively proportional to the length of the beam and positively proportional to the initial height of the beam. That means the higher the initial height and the shorter the beam, the greater the overload power. According to Figure 3, it is clear that when the beam length is 200 μm and the initial height of the beam is 2 μm, the overload power reaches the maximum value of 3.54 W. However,

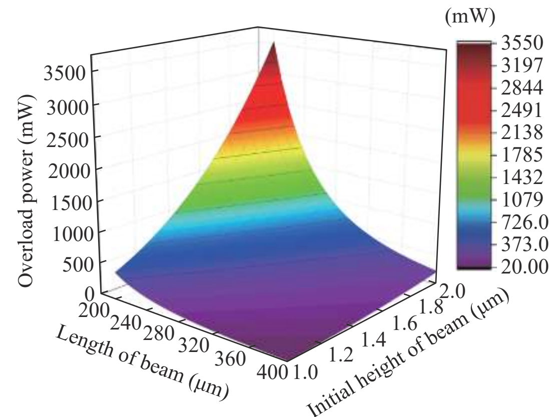

Figure 3 The relationship between overload power and the length and initial height of the beam ($t = 2$ μm).

if the initial height of beam is designed too high, it will result in the electrostatic attraction between the signal line and the cantilever beam becoming smaller. Thus the amount of capacitance change will become smaller and difficult to measure.

2. Sensitivity analysis

For the sensitivity of the capacitive power sensor, the capacitance between the beam and the measuring electrode can be seen as the integral of an infinite number of parallel plate capacitors from the left end to the right end of the measuring electrode [13], as shown in (18).

$$C_2 = \int_{x_1}^{x_2} \frac{\varepsilon_0 b_2}{g_0 - \frac{x}{L}\delta} \mathrm{d}x = \int_{c_1}^{c_2} \frac{\varepsilon_0 b_2 L}{g_0 - a\delta} \mathrm{d}a \tag{18}$$

where b_2 is the width of measuring electrode ($b_1 < b_2$).

The initial capacitance between the beam and the measuring electrode is a standard flat plate capacitor, the capacitance of which can be expressed as (19). The sensitivity of capacitive power sensor is the ratio of the change in capacitance between the measuring electrode and the beam to the input power as shown in (20).

$$C_{2_0} = \frac{\varepsilon_0 b_2 (x_2 - x_1)}{g_0} = \frac{\varepsilon_0 b_2 (c_2 - c_1) L}{g_0} \tag{19}$$

$$\begin{aligned} S_1 &= \frac{\Delta C_2}{P_{\text{in}}} = \frac{C_2 - C_{2_0}}{P_{\text{in}}} \\ &= \frac{0.458 Z_0 \varepsilon_0^2 b_2 L^5}{(1 - c_3) E t^3 \delta} \cdot \left[\int_{c_1}^{c_2} \frac{1}{g_0 - a\delta} \mathrm{d}a - \frac{c_2 - c_1}{g_0} \right] \\ &\quad \cdot \int_{c_3}^{1} \frac{f_2(a)}{(g_0 - \delta f_2(a))^2} \mathrm{d}a \end{aligned} \tag{20}$$

It shows that the sensitivity of the capacitive power sensor is closely related to the width of the measuring electrode, and the length, thickness, initial height of the cantilever beam. Figure 4 shows the relationship of sensitivity with the width of the measuring electrode and the length of the beam as the initial height of the beam is 1.6 μm. The sensitivity is proportional to the length of the beam and proportional to the width of the measuring electrode. The wider the measuring electrode and the longer the beam, the larger the sensitivity. When the length of the beam is 400 μm and the width of the measuring electrode is 300 μm, the sensitivity reaches the maximum value of 353.52 fF/W. Considering the overload power, the cantilever beam should not be designed too long, so that the overload power of the sensor will become small, and the beam is easy to collapse; nor should it be designed too short, so that the sensitivity of the sensor will become poor. Therefore, it is necessary to fully consider the output characteristics of the sensor, and reasonably design the cantilever length, initial height and width of the measuring electrode.

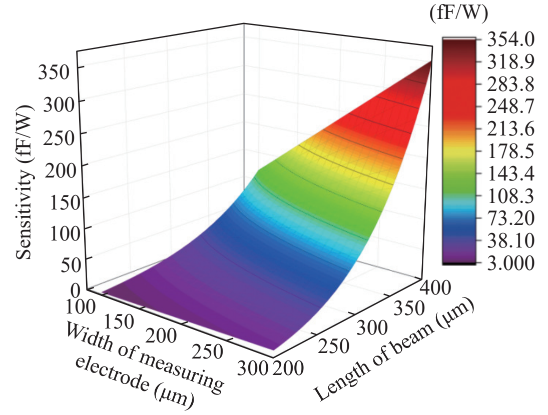

Figure 4 The relationship between sensitivity and the length of beam and the width of test electrode (t = 2 μm).

The structural parameters of thermoelectric detection channel are shown in Table 2, and its sensitivity [15] is expressed as (21).

$$S_2 = \frac{|\alpha_n - \alpha_p| N}{\lambda_e p W d_e} \cdot \frac{\sinh(pl)}{\cosh(p(l + l_0))} \tag{21}$$

where α_n is the Seebeck coefficient of n^+GaAs, α_p is the Seebeck coefficient of Au, N is the number of thermocouples, l is the thermopile length, l_0 is the distance between the load resistance and the hot end of thermopiles, and W is the effective width of the heat flow. d_e and λ_e are expressed as (22), and represent the equivalent thickness of the thermopile and equivalent thermal conductivity, respectively.

Table 2 Structural parameters of thermoelectric detection channel

Symbol	Description	Value
λ_p	Thermal conductivity of n+GaAs	46 W/(m·K)
λ_n	Thermal conductivity of Au	315 W/(m·K)
λ_s	Thermal conductivity of GaAs substrate	46 W/(m·K)
ε_p	Radiation coefficient of n+GaAs	0.3
ε_n	Radiation coefficient of Au	0.02
ε_s	Radiation coefficient of GaAs substrate	0.3
d_t	Thickness of thermopile	0.3 μm
d_s	Thickness of GaAs substrate	100 μm
α_p	Seebeck coefficient of n+GaAs	100 μV/K
α_n	Seebeck coefficient of Au	1.7 μV/K
T_0	Ambient temperature	300 K
σ_b	Stefan-Boltzmann constant	5.67×10^{-8} W/(m^2·K^4)
W	Effective width of heat flow	274 μm
h	Convection coefficient	1 W/(m^2·K)
l	Length of thermocouple	100 μm
l_0	Distance from thermocouples heat end to load resistance	10 μm
N	Number of thermocouples	12

$$\begin{cases} d_e = d_s + \dfrac{d_t}{2} \\ \lambda_e = \dfrac{\lambda_s d_s + \lambda_t (d_t/2)}{d_e} = \dfrac{\lambda_s d_s + \lambda_t (d_t/2)}{d_s + d_t/2} \\ \lambda_t = \dfrac{\lambda_n + \lambda_p}{2} \end{cases} \tag{22}$$

where d_s and d_t denote the thickness of GaAs substrate and thermocouple arm, respectively, λ_s and λ_t denote the thermal conductivity of GaAs substrate and thermocouple arm, respectively, and λ_n and λ_p denote the thermal conductivity of Au and n^+GaAs, respectively. The p in (20) is expressed as (23).

$$\begin{cases} p = \sqrt{\dfrac{H}{\lambda_e d_e}} \\ H = 2h + 4\sigma_b (\varepsilon_e + \varepsilon_s) T_0^3 \\ \varepsilon_e = \dfrac{\varepsilon_n + \varepsilon_p}{2} \end{cases} \tag{23}$$

where T_0 is the ambient temperature, σ_b is the Stefan-Boltzmann constant, h is the convection coefficient, and ε_p, ε_n, and ε_s denote the radiation coefficients of n^+GaAs, Au, and GaAs substrates, respectively.

III. Fabrication

The dual-channel microwave power sensor with MEMS cantilever beam structure constructed in this paper is fabricated by MEMS technology and GaAs MMIC technology. GaAs material has higher electron mobility and wider band gap, so it is chosen as the substrate material. As shown in Figure 5 (the SEM photo is shown in Figure 6), the fabrication process steps are as follows:

a) An undoped GaAs epitaxial wafer is chosen with a thickness of 600 μm as the substrate, and an n^+GaAs epitaxial layer is formed on the surface of the substrate by ion implantation.

b) The semiconductor thermocouple arm is formed by patterning and etching the n^+GaAs epitaxial layer. TaN is performed photolithography, sputtered, and peeled to form terminal resistance.

c) AuGeNi/Au with a thickness of 3000 Å is performed photolithography and sputtered to form metal thermocouple arms, CPW, test electrode, and anchor zones.

d) Silicon nitride with a thickness of 1000 Å is deposited by PECVD.

e) A 1.6 μm polyimide sacrificial layer is sputtered by spin coating.

f) A 2300 Å of the underlying Au is evaporated and photoetched. Plate on 2 μm Au and remove photoresist. Reverse lithography of the Au layer to etch the underlying Au and form a through-hole structure on the MEMS beam.

g) Form a MEMS cantilever beam by releasing the polyimide sacrificial layer and remove the remaining water with absolute ethanol.

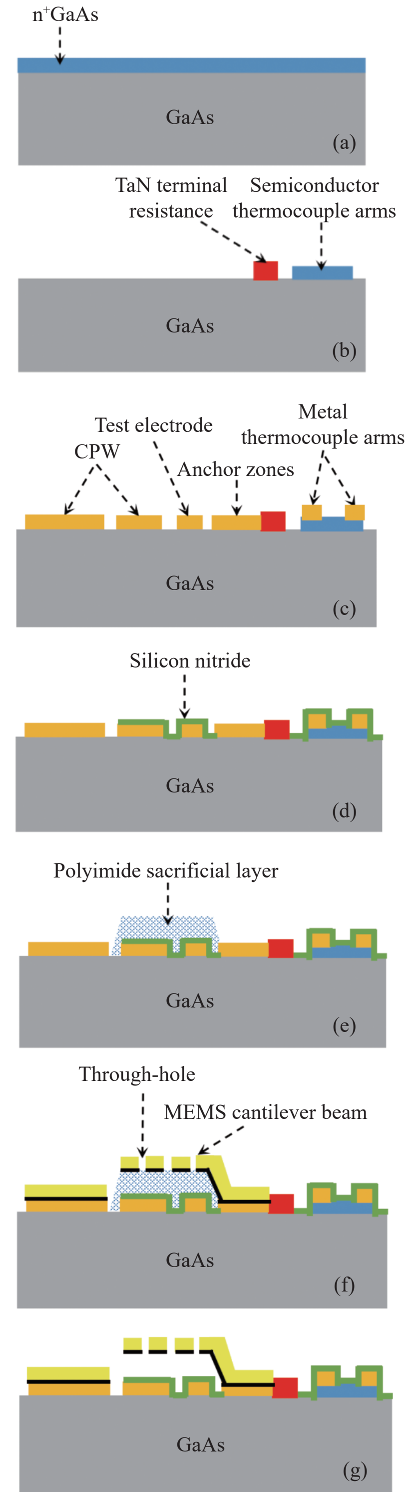

Figure 5 Process steps of fabrication.

IV. Measurements and Discussions

The measurement setup of MEMS dual-channel microwave power sensor is shown in Figure 7. The Agilent E8257D signal generator provides microwave signals. When the input microwave power is low, it is measured by the thermoelectric channel through measuring the output voltage with a Fluke 450 multimeter. When the

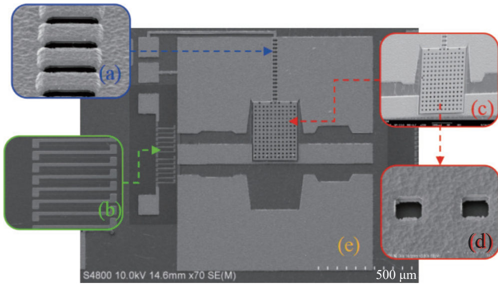

Figure 6 SEM photo. (a) Anchor area; (b) Thermopile; (c) Cantilever beam; (d) Air gap; (e) Microwave power sensor manufactured.

input microwave power is high, it is measured by capacitive microwave power sensors through measuring the output capacitance on the AD7747 evaluation board of the analog device.

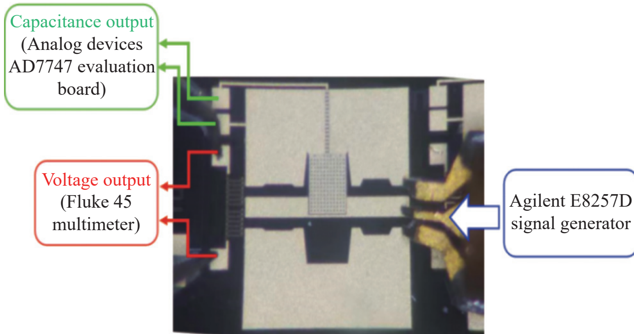

Figure 7 Microwave power test framework.

1. Output voltage measurement

The measurement results and theoretical calculation results of microwave power of thermoelectric channel are shown in Figure 8, the theoretical sensitivity is 0.093 V/W, while the measured sensitivity is about 0.11 V/W, and the error is about 18.28%. The error may be due to the uneven heating of the hot end of the thermopile, and the effective width of the heat flow is small in the measurement. The sensitivity of thermoelectric sensors is compared as shown in Table 3.

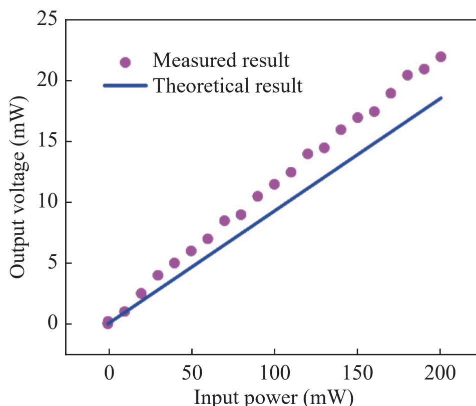

Figure 8 Comparison between measured result and theoretical result of output voltage of thermoelectric channel.

Table 3 Comparison of sensitivity of thermoelectric sensor

Reference	Number of thermocouples	Normalization of the number of thermocouples	Sensitivity (mV/W)
[6]	10	0.7143	82.5
[16]	14	1	109
[21]	12	0.8571	71.7
[22]	14	1	8.7
This work	12	0.8571	110

2. Output capacitance measurement

Figure 9 shows the theoretical results of the three models and the measured results of capacitive microwave power. The measured sensitivity is 65.17 fF/W. The theoretical sensitivity with the lumped model is 92.93 fF/W, which is a large error from the measured value, and the relative error is about 42.6%. The theoretical sensitivity with the pivot model is 50.88 fF/W, which is small and the measured value is small, and the relative error is about 28.1%. The theoretical sensitivity with the deflection model proposed in this work is 75.21 fF/W, which is smaller than the measured value, and the relative error is about 13.3%. The accuracy of deflection model is improved by 29.3% compared with lumped model and 14.8% compared with pivot model. This shows that the deflection model has higher accuracy in the capacitive microwave power sensors. The sensitivity of capacitive sensors is compared as shown in Table 4.

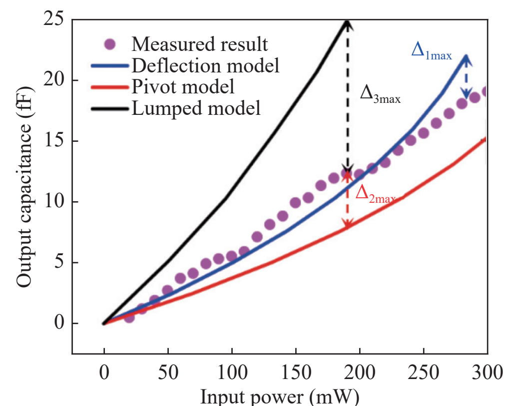

Figure 9 Comparison between measured result and theoretical result of output capacitance of capacitive channel.

V. Conclusion

In order to better study the output characteristics of capacitive MEMS microwave power sensor, a static deflection model is proposed in this work, and theoretically studies the overload power and sensitivity of the sensor. A MEMS dual-channel microwave power sensor is designed, and its manufacturing process is described in this work. The output voltage and output capacitance are measured, and the theoretical value is compared with the measured value. It is found that for capacitive power

Table 4 Comparison of sensitivity of capacitive sensors

Reference	Types of beam	Size of beam (μm × μm)	Sensitivity (fF/W)
[10]	Fixed beam	400 × 200	20
[12]	Fixed beam	380 × 110	2.86
[14]	Double cantilever beam	189 × 50	51.6
[16]	Cantilever beam	200 × 50	24
[23]	Cantilever beam	125 × 85	2.8
This work	Cantilever beam	308 × 240	65.17

sensor, the deflection model proposed in this work has a smaller relative error and higher accuracy than the traditional lumped model and pivot model.

Acknowledgements

This work was supported by the National Natural Science Foundation of China (Grant No. 61904089), the Province Natural Science Foundation of Jiangsu (Grant No. BK20190731), the China Postdoctoral Science Foundation (Grant No. 2017M621692), and Student's Platform for Innovation and Entrepreneurship Training Program (Grant No. 202210293012Z).

References

[1] U. Baehr, M. Freier, M. Lewis, *et al.*, "Frequency induced stiction for MEMS accelerometers," *Journal of Microelectromechanical Systems*, vol. 29, no. 3, pp. 285–295, 2020.

[2] M. Ozdogan, S. Towfighian, and R. N. Miles, "Modeling and characterization of a pull-in free MEMS microphone," *IEEE Sensors Journal*, vol. 20, no. 12, pp. 6314–6323, 2020.

[3] A. Dehé, V. Krozer, K. Fricke, *et al.*, "Integrated microwave power sensor," *Electronics Letters*, vol. 31, no. 25, pp. 2187–2188, 1995.

[4] D. B. Wang and X. P. Liao, "A terminating-type MEMS microwave power sensor and its amplification system, " *Journal of Micromechanics and Microengineering*, vol. 20, no. 7, article no. 075021, 2010.

[5] Z. Q. Zhang, X. P. Liao, and X. H. Wang, "Research on thermocouple distribution for microwave power sensors based on GaAs MMIC process," *IEEE Sensors Journal*, vol. 15, no. 8, pp. 4178–4179, 2015.

[6] C. L. Chu and X. P. Liao, "X-band monolithic microwave integrated detector based on MEMS thermoelectric power sensor," *IEEE Sensors Letters*, vol. 3, no. 12, article no. 3502804, 2019.

[7] J. H. Li, X. P. Liao, and C. L. Chu, "A new RF MEMS power sensor based on double-deck thermocouples with high sensitivity and large dynamic range," *IEEE Microwave and Wireless Components Letters*, vol. 31, no. 8, pp. 1023–1026, 2021.

[8] J. H. Li and X. P. Liao, "An X-band microwave thermoelectric power detector in 0.18-μm CMOS technology," in *Proceedings of the 2022 IEEE Sensors*, Dallas, USA, pp. 1–4, 2022.

[9] L. J. Fernández, R. J. Wiegerink, J. Flokstra, *et al.*, "A capacitive RF power sensor based on MEMS technology," *Journal of Micromechanics and Microengineering*, vol. 16, no. 7, pp. 1099–1107, 2006.

[10] Y. Cui, X. P. Liao, and Z. Zhu, "A novel microwave power sensor using MEMS fixed-fixed beam," in *Proceedings of the Sensors, 2021 IEEE*, Limerick, Ireland, pp. 1305–1308, 2011.

[11] Z. X. Yi, X. P. Liao, and Z. Zhu, "An 8–12GHz capacitive power sensor based on MEMS cantilever beam, " in *Proceedings of the Sensors, 2011 IEEE*, Limerick, Ireland, pp. 1958–1961, 2011.

[12] H. Yan and X. P. Liao, "The high power up to 1 W characteristics of the capacitive microwave power sensor with grounded MEMS beam," *IEEE Sensors Journal*, vol. 15, no. 12, pp. 6765–6766, 2015.

[13] W. Zuo, Q. T. Guo, X. C. Ji, *et al.*, "Structural optimization of capacitive MEMS microwave power sensor," *IEEE Sensors Journal*, vol. 20, no. 19, pp. 11380–11386, 2020.

[14] C. Li, J. J. Xiong, and D. B. Wang, "A novel capacitive microwave power sensor based on double MEMS cantilever beams," *IEEE Sensors Journal*, vol. 22, no. 12, pp. 11803–11809, 2022.

[15] D. B. Wang, X. P. Liao, and T. Liu, "A novel thermoelectric and capacitive power sensor with improved dynamic range based on GaAs MMIC technology," *IEEE Electron Device Letters*, vol. 33, no. 2, pp. 269–271, 2012.

[16] D. B. Wang and X. P. Liao, "A novel MEMS double-channel microwave power sensor based on GaAs MMIC technology," *Sensors and Actuators A: Physical*, vol. 188 pp. 95–102, 2012.

[17] P. Kosobutskyy, A. Kovalchuk, M. Szermer, *et al.*, "Statistical optimization of the cantilever beams," in *Proceedings of the Experience of Designing and Application of CAD Systems in Microelectronics*, Lviv, Ukraine, pp. 245–247, 2015.

[18] Z. X. Yi and X. P. Liao, "A cascaded terminating-type and capacitive-type power sensor for -10- to 22-dBm application," *IEEE Electron Device Letters*, vol. 37, no. 4, pp. 489–491, 2016.

[19] P. V. Kasambe, A. Barwaniwala, B. Sonawane, *et al.* , "Mathematical modeling and numerical simulation of novel cantilever beam designs for ohmic RF MEMS switch application, " in *Proceedings of the 2019 International Conference on Advances in Computing, Communication and Control*, Mumbai, India, pp. 1–6, 2019.

[20] A. D. Singh and R. M. Patrikar, "Development of nonlinear electromechanical coupled macro model for electrostatic MEMS cantilever beam," *IEEE Access*, vol. 7, pp. 140596–140605, 2019.

[21] Z. Q. Zhang, Y. Guo, F. Li, *et al.*, "A sandwich-type thermoelectric microwave power sensor for GaAs MMIC-compatible applications," *IEEE Electron Device Letters*, vol. 37, no. 12, pp. 1639–1641, 2016.

[22] C. H. Cai, L. D. Wei, X. Wu, *et al.*, "A novel gradient thermoelectric microwave power sensors based on GaAs MMIC technology," *Microsystem Technologies*, vol. 27, no. 1, pp. 243–249, 2021.

[23] J. H. Li and X. P. Liao, "High-power electro-mechanical behavior of a capacitive microwave power sensor with warped cantilever beam," *Solid-State Electronics*, vol. 172, article no. 107877, 2020.

Ye JIN was born in 2002. She is studying at Nanjing University of Posts and Telecommunications, Nanjing, China, for her undergraduate degree. Her research interest is MEMS microwave power sensor.
(Email: 1059831817@qq.com)

Debo WANG was born in 1983. He received the B.S. degree in electronic science and technology from Hebei University of Science and Technology, Shijiazhuang, China, in 2007, the M.S. degree and the Ph.D. degree from the Key Laboratory of MEMS of the Ministry of Education, Southeast University, Nanjing, China, in 2010 and 2012. He is now a Post-Doctor at Nanjing University, Nanjing, China, and an Associate Professor at Nanjing University of Posts and Telecommunication, Nanjing, China. The discipline of his research focuses on the RF MEMS devices, particularly on microwave power sensor and its package.
(Email: wdb@njupt.edu.cn)